Research Article

Journal of PeptideScience

Received: 16 March 2012 Revised: 18 April 2012 Accepted: 20 April 2012 Published online in Wiley Online Library: 22 May 2012

(wileyonlinelibrary.com) DOI 10.1002/psc.2418

Conformations of helical Aib peptides containing a pair of L-amino acid and D-amino acid

Yosuke Demizu,[a]* Yu-u Yabuki,[a] Mitsunobu Doi,[b] Yukiko Sato,[a] Masakazu Tanaka[c] and Masaaki Kurihara[a]*

A pair of L-leucine (L-Leu) and D-leucine (D-Leu) was incorporated into α-aminoisobutyric acid (Aib) peptide segments. The dominant conformations of four hexapeptides, Boc-L-Leu-Aib-Aib-Aib-Aib-L-Leu-OMe (1a), Boc-D-Leu-Aib-Aib-Aib-Aib-L-Leu-OMe (1b), Boc-Aib-Aib-L-Leu-L-Leu-Aib-Aib-OMe (2a), and Boc-Aib-Aib-D-Leu-L-Leu-Aib-Aib-OMe (2b), were investigated by IR, ^{1}H NMR, CD spectra, and X-ray crystallographic analysis. All peptides 1a,b and 2a,b formed 3_{10}-helical structures in solution. X-ray crystallographic analysis revealed that right-handed (*P*) 3_{10}-helices were present in 1a and 1b and a mixture of right-handed (*P*) and left-handed (*M*) 3_{10}-helices was present in 2b in their crystalline states. Copyright © 2012 European Peptide Society and John Wiley & Sons, Ltd.

Keywords: α-aminoisobutyric acid; amino acids; peptide; helical structure; X-ray crystallography

Introduction

α-Helices in natural peptides and proteins have a right-handed (*P*) screw sense, because they are composed of L-α-amino acids (L-AA) with an α-chiral center [1]. Synthetically stabilized helical peptides are widely used in a variety of fields such as organic and biological chemistry [2–7]. In particular, α-aminoisobutyric acid (Aib) has been utilized for the construction of helical peptides. However, Aib is an achiral amino acid and does not induce helical screw handedness. To date, several studies have attempted to control the helical screw sense of Aib-based oligopeptides [8–18]. Furthermore, the screw sense control of helical Aib-based peptides using a single chiral AA at the N-terminus or C-terminus has been investigated in the past decade [19–33]. Recently, we reported that the hexapeptide Boc-L-Leu-L-Leu-Aib-D-Leu-D-Leu-Aib-OMe [*tert*-butoxycarbonyl (Boc), L-leucine (L-Leu), D-leucine (D-Leu), methyl ester (OMe)], which has two L-Leu, two D-Leu, and two achiral Aib, could form a left-handed (*M*) 3_{10}-helical structure in the crystalline state [34,35]. Furthermore, we have investigated the preferred conformations of L-Leu-L-Leu-Aib-L-Leu-L-Leu-Aib peptides by substituting an L-Leu with a D-Leu and revealed that the D-Leu-substitution site influenced the peptide's secondary structure [36]. In their crystalline structures, the replacement of the sequence with D-Leu (1) or D-Leu(2) residues did not have a significant effect on the right-handed helical screw sense. On the other hand, the replacement of the sequence with D-Leu(4) or D-Leu(5) residues had great influences on the peptide secondary structures to induce left-handed helical screw sense. Therefore, we are attracted to investigating the influence of a pair of L-AA and D-AA residues to Aib-based helical peptides. Herein, we designed and synthesized four hexapeptides, Boc-L-Leu-Aib-Aib-Aib-Aib-L-Leu-OMe (**1a**) having an N-terminal L-Leu and a C-terminal L-Leu, Boc-D-Leu-Aib-Aib-Aib-Aib-L-Leu-OMe (**1b**) having an N-terminal D-Leu and a C-terminal L-Leu, Boc-Aib-Aib-L-Leu-L-Leu-Aib-Aib-OMe (**2a**) having a central L-Leu-L-Leu segment, and Boc-Aib-Aib-D-Leu-L-Leu-Aib-Aib-OMe (**2b**) having a central D-Leu-L-Leu segment. Then, we analyzed their conformations in solution and in the crystalline state (Figure 1).

Materials and Methods

Synthesis and Characterization of Peptides

Preparation of peptides **1a**,**b** and **2a**,**b** was performed by conventional solution-phase methods using a segment condensation strategy with *O*-benzotriazole-*N*,*N*,*N*′,*N*′-tetramethyluronium hexafluorophosphate and HOBt as coupling reagents. All compounds were purified by column chromatography on silica gel. The spectroscopic data of **1a**,**b** and **2a**,**b** supported the following structures (Figure 2).

*Boc-L-Leu-Aib-Aib-Aib-Aib-L-Leu-OMe (**1a**)*

Colorless crystals; mp 200–202 °C; $[\alpha]_D^{21} = -26.2$ (*c* 1.10, $CHCl_3$); IR (ATR): ν 3336, 2962, 2871, 1672, 1526 cm^{-1}; ^{1}H NMR (400 MHz, $CDCl_3$) δ 7.61 (d, $J = 8.4$ Hz, 1H), 7.46 (br s, 1H), 7.33 (br s, 1H), 7.19 (br s, 1H), 6.40 (br s, 1H), 4.99 (d, $J = 3.60$ Hz, 1H), 4.58 (m, 1H), 3.83 (m, 1H), 3.68 (s, 3H), 1.84–1.88 (m, 2H), 1.43–1.82 (m, 37H), 0.90–1.00 (m, 12H) ^{13}C NMR (100 MHz, $CDCl_3$) δ 175.9, 175.0, 174.2, 174.1, 173.6, 173.3, 156.5, 80.6, 56.9, 56.8, 56.8, 56.5, 54.7, 51.8, 51.1, 40.2, 39.5, 28.3, 25.8, 25.3, 24.8, 24.7, 24.4, 23.0, 22.9, 21.7, 21.4; [HR–ESI(+)]: *m/z* calcd for $C_{34}H_{62}N_6O_9Na$ $[M + Na]^+$ 721.4476; found, 721.4499.

* *Correspondence to: Yosuke Demizu and Masaaki Kurihara, Division of Organic Chemistry, National Institute of Health Sciences, 1-18-1, Kamiyoga, Setagaya, Tokyo 158-8501, Japan. E-mail: demizu@nihs.go.jp; masaaki@nihs.go.jp*

a *Division of Organic Chemistry, National Institute of Health Sciences, 1-18-1, Kamiyoga, Setagaya, Tokyo 158-8501, Japan*

b *Osaka University of Pharmaceutical Sciences, Osaka 569-1094, Japan*

c *Graduate School of Biomedical Sciences, Nagasaki University, 1-14 Bunkyo-machi, Nagasaki 852-8521, Japan*

Journal of PeptideScience

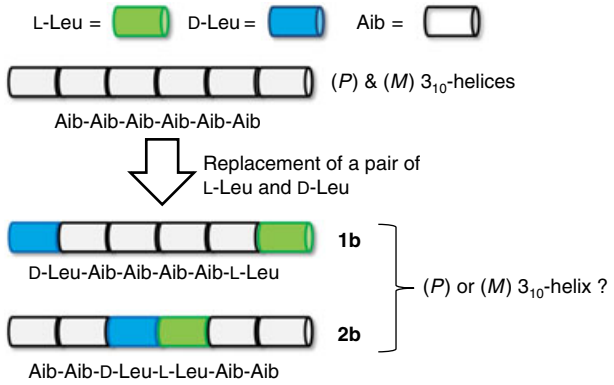

Figure 1. Design of hexapeptides **1b** and **2b** with a pair of L-Leu and D-Leu residues.

*Boc-D-Leu-Aib-Aib-Aib-Aib-L-Leu-OMe (**1b**)*

Colorless crystals; mp 223–225 °C; $[\alpha]_D^{21} = -22.8$ (*c* 1.00, $CHCl_3$); IR (ATR): ν 3335, 2962, 2871, 1672, 1527 cm^{-1}; ^1H NMR (400 MHz, $CDCl_3$) δ 7.61 (d, *J* = 8.0 Hz, 1H), 7.51 (br s, 1H), 7.40 (br s, 1H), 7.30 (br s, 1H), 6.46 (br s, 1H), 5.01 (d, *J* = 2.8 Hz, 1H), 4.58 (m, 1H), 3.86 (m, 1H), 3.66 (s, 3H), 1.83–1.91 (m, 2H), 1.39–1.73 (m, 37H), 0.92–1.00 (m, 12H) ^{13}C NMR (100 MHz, $CDCl_3$) δ 175.7, 174.7, 174.0, 173.9, 173.8, 172.8, 156.5, 81.2, 56.9, 56.9, 56.8, 56.4, 55.1, 51.7, 51.0, 40.4, 39.8, 28.2, 27.1, 26.5, 26.3, 24.9, 24.3, 24.0, 23.7, 23.5, 23.1, 22.7, 21.8, 21.4; [HR–ESI(+)]: *m/z* calcd for $C_{34}H_{62}N_6O_9Na$ $[M + Na]^+$ 721.4476; found, 721.4485.

*Boc-Aib-Aib-L-Leu-L-Leu-Aib-Aib-OMe (**2a**)*

Colorless crystals; mp 208–210 °C; $[\alpha]_D^{21} = -10.0$ (*c* 0.90, $CHCl_3$); IR (ATR): ν 3334, 2961, 2872, 1670, 1525 cm^{-1}; ^1H NMR (400 MHz, $CDCl_3$) δ 7.58–7.62 (m, 2H), 7.06 (br s, 1H), 6.97 (br s, 1H), 6.88 (br s, 1H), 5.75 (br s, 1H), 4.23 (m, 1H), 4.12 (m, 1H), 3.65 (s, 3H), 1.59–1.80 (m, 6H), 1.37–1.51 (m, 33H), 0.85–0.95 (m, 12H); ^{13}C NMR (100 MHz, $CDCl_3$) δ 175.9, 175.5, 175.3, 174.4, 174.1, 172.6, 155.9, 81.0, 56.9, 56.8, 56.5, 55.8, 54.5, 53.2, 52.1, 39.9, 39.5, 28.3, 28.2, 27.9, 27.0, 26.3, 25.3, 25.0, 24.9, 24.7, 24.4, 23.3, 23.1, 23.0, 21.1, 20.9; [HR–ESI(+)]: *m/z* calcd for $C_{34}H_{62}N_6NaO_9$ $[M + Na]^+$ 721.4476; found, 721.4505.

*Boc-Aib-Aib-D-Leu-L-Leu-Aib-Aib-OMe (**2b**)*

Colorless crystals; mp 197–198 °C; $[\alpha]_D^{21} = -1.8$ (*c* 1.10, $CHCl_3$); IR (ATR) ν 3334, 2960, 2871, 1671, 1523 cm^{-1}; ^1H NMR (400 MHz, $CDCl_3$) δ 7.79 (d, *J* = 6.8 Hz, 1H), 7.71 (d, *J* = 6.0 Hz, 1H), 7.23 (br s, 1H), 6.91 (br s, 1H), 6.57 (br s, 1H), 5.05 (br s, 1H), 4.27 (m, 1H), 4.13 (m, 1H), 3.69 (s, 3H), 1.81–1.88 (m, 2H), 1.72–1.77 (m, 4H), 1.61–1.43 (m, 33H), 0.88–0.95 (m, 12H); ^{13}C NMR (100 MHz, $CDCl_3$) δ 175.3, 175.1, 174.8, 174.2, 173.6, 172.2, 156.0, 81.1, 56.8, 56.8, 56.7, 55.7, 54.0, 53.0, 52.0, 38.7, 38.2, 28.2, 28.1, 27.8, 27.0, 26.2, 25.2, 25.2, 24.9, 24.8, 24.6, 24.3, 23.3, 23.0, 23.0, 21.1, 20.9, 20.9; [HR–ESI(+)]: *m/z* calcd for $C_{34}H_{62}N_6O_9Na$ $[M + Na]^+$ 721.4476; found, 721.4466.

Conformational Analysis of Peptides

It is thought to be best to analyze the conformations of peptides by using the same solvent, but it would be difficult. For example, in the case of CD spectra, it is not able to use $CHCl_3$ as a solvent under 250 nm because of noise and high background signals. In the case of X-ray, it is somewhat difficult to give suitable crystals for analysis with the use of the desirable solvent (we attempted to crystallize using various solvents). Therefore, we measured the conformations of peptides in different solvents.

FT-IR Spectra

FT-IR spectra were recorded on a JASCO FT/IR-4100 spectrometer (JASCO, Tokyo, Japan) at 24 °C, with a resolution of 1.0 cm^{-1}, an average of 64 scans used for the solution ($CDCl_3$) method and a 0.1-mm path length used for NaCl cells.

^1H NMR Spectra

^1H NMR spectra were recorded on a Varian AS 400 spectrometer (Agilent, CA, USA) at 24 °C. Measurements were carried out in $CDCl_3$ with tetramethylsilane used as an internal standard.

CD Spectra

CD spectra were recorded with a Jasco J-720W spectropolarimeter using a 1.0-mm path length cell. The data were expressed in terms of $[\theta]_M$, the total molar ellipticity (deg cm^2 $dmol^{-1}$). 2,2,2-Trifluoroethanol (TFE) was used as a solvent.

X-ray Diffraction

Peptides **1a**, **1b**, and **2b** became good crystals for X-ray crystallographic analysis by slow evaporation of solvents DMF/H_2O for **1a** and **2b** and MeOH/H_2O for **1b** at room temperature. Although we attempted to crystallize for peptide **2a** with the use of various solvents (MeOH, EtOH, *i*PrOH, DMF, DMSO, H_2O, $CHCl_3$, CH_2Cl_2, AcOEt, acetone, Et_2O, THF, 1,4-dioxane, hexane, toluene, benzene,

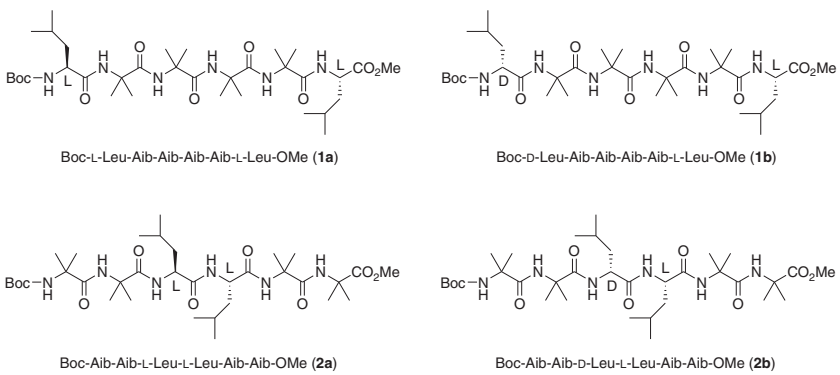

Figure 2. Chemical structures of hexapeptides **1a**, **1b**, **2a**, and **2b**.

and a mixture of them), we could not obtain suitable crystals. The crystal and diffraction parameters of **1a**, **1b**, and **2b** are summarized in Table 1. Data collection was performed on Bruker AXS SMART APEX (Bruker, Karlsruhe, Germany) imaging plate diffractometers using graphite-monochromated Mo Kα radiation. All crystals remained stable during the X-ray data collection. The structures of **1a**, **1b**, and **2b** were solved by the direct method using SHELXS 97 [37] and expanded by the Fourier technique using SHELXL 97 [38]. All non-H atoms were given anisotropic thermal parameters, some H-atoms were refined isotropically, and the remaining H-atoms were given at the calculated positions. The final cycle of full-matrix least-squares refinement of **1a** gave an R_1 factor of 0.0489 based on 4618 ($I > 2\sigma(I)$) reflections and an R_w factor of 0.1426 for all data. The R_1 factor of **1b** was 0.0543 based on 4520 ($I > 2\sigma(I)$) reflections and an R_w factor of 0.1623 for all data. The R_1 factor of **2b** was 0.0704 based on 8308 ($I > 2\sigma(I)$) reflections and an R_w factor of 0.2150 for all data. CCDC-808947 for **1a**, CCDC-8035009 for **1b**, and CCDC-803510 for **2b** contain the supplementary crystallographic data for this paper. These data can be obtained free of charge at www.ccdc.cam.ac.uk/conts/retrieving.html (or from the Cambridge Crystallographic Data Centre, 12, Union Road, Cambridge CB2 1EZ, UK; fax: (+44) 1223-336-033 or deposit@ccdc.cam.ac.uk. Relevant backbone and side chain torsion angles and the intramolecular and intermolecular hydrogen-bond parameters are listed in Tables 2 and 3.

Results and Discussion

FT-IR Spectra

Figure 3 shows the IR absorption spectra of peptides **1a**,**b** and **2a**,**b** in the 3250–3500 cm^{-1} region at a peptide concentration of 1.0 mM in $CDCl_3$ solution. In the IR absorption spectra of peptides **1a**,**b** and **2a**,**b**, the weak band in the 3420 cm^{-1} region was assigned to free peptide NH groups and the strong band at 3330 cm^{-1} was assigned to peptide NH groups with N–H···O=C intramolecular hydrogen bonds. These IR spectra are very similar to those of Aib homopeptides, which form 3_{10}-helices in solution [39].

Table 2. Selected torsion angles ω, ϕ, ψ, and χ^a (°) for **1a**, **1b**, and **2b**, as determined by X-ray crystallographic analysis

Torsion angle	1a	1b	2b	
			A	B
ω_0	−175.9	178.8	−157.3	153.6
ϕ_1	−67.7	−48.8	−62.0	64.1
ψ_1	−17.8	−38.6	−49.8	44.3
ω_1	172.7	−176.5	−174.7	172.6
ϕ_2	−47.7	−50.9	−56.0	56.7
ψ_2	−33.5	−33.1	−31.9	33.9
ω_2	−175.3	−174.6	−177.2	175.5
ϕ_3	−50.0	−51.3	−53.9	69.3
ψ_3	−39.8	−41.7	−35.7	17.4
ω_3	−173.5	−172.9	−175.4	173.9
ϕ_4	−62.8	−63.6	−70.5	56.6
ψ_4	−21.2	−21.0	−22.6	36.7
ω_4	177.4	176.6	173.8	177.2
ϕ_5	−57.1	−57.9	−57.2	62.1
ψ_5	−35.0	−31.8	−41.9	40.6
ω_5	−170.9	−169.2	−173.4	171.3
ϕ_6	−80.5	−83.2	53.3	−49.3
ψ_6	−20.1	−20.3	33.0	−35.0
ω_6	−178.9	−178.3	178.6	−180.0
χ_1	−74.9	57.8	—	—
χ_3	—	—	60.2	69.0
χ_4	—	—	−64.1	−65.4
χ_6	−54.4	−54.5	—	—

[a]The torsion angle χ means side chain torsion angles of Leu residues.

Table 1. Crystal and diffraction parameters of peptides **1a**, **1b**, and **2b**

	1a	1b	2b
Formula	$C_{34}H_{62}N_6O_9$	$C_{34}H_{62}N_6O_9$	$C_{34}H_{62}N_6O_9$
M_r	698.90	698.90	698.90
Crystal dimensions (mm)	0.40 × 0.25 × 0.25	0.45 × 0.25 × 0.20	0.30 × 0.30 × 0.05
Crystal system	Monoclinic	Monoclinic	Triclinic
Lattice parameters			
a (Å)	9.621	9.680	10.544
b (Å)	19.850	19.690	19.690
c (Å)	10.941	10.698	10.178
α (°)	90	90	81.380
β (°)	102.187	101.152	83.998
γ (°)	90	90	88.394
V (Å^3)	2042.4	2000.5	2081.8
Space group	$P2_1$	$P2_1$	$P1$
Z value	2	2	2
D_{calc} (g/cm^3)	1.14	1.16	1.12
μ (Mo Kα) (cm^{-1})	0.82	0.85	0.81
No. of observations	4618 ($I > 2\sigma(I)$)	4520 ($I > 2\sigma(I)$)	8308 ($I > 2\sigma(I)$)
No. of variables	442	442	883
R_1, R_w	0.0489, 0.1426	0.0543, 0.1623	0.0704, 0.2150
Solvent	DMF/H_2O	MeOH/H_2O	DMF/H_2O

Journal of PeptideScience

^{1}H NMR Spectra

In the ^{1}H NMR spectra of **1a**,**b** and **2a**,**b**, N(1)H proton signals of the urethane type at the N-terminus were unambiguously determined by their high-field positions at δ 4.93 (br s, 1H) in **1a**, δ 5.01 (br s, 1H) in **1b**, δ 4.93 (br s, 1H) in **2a**, and δ 5.05 (br s, 1H) in **2b**, but the remaining five peptide NH protons could not be assigned at this stage. Figure 4 shows the solvent perturbation experiment involving the addition of the strong H-bond acceptor solvent DMSO (0–10% (v/v)). Two NH chemical shifts in all peptides **1a**,**b** and **2a**,**b** were sensitive to the addition of the perturbing reagent DMSO. These results are in accord with a 3_{10}-helical structure, in which two NH groups at the N-terminus of the peptide are freely solvated.

Figure 5(A)–(D) shows the 2D NOESY ^{1}H NMR spectra of **1a**, **1b**, **2a**, and **2b** in $CDCl_3$ solution, respectively. The spectra of **1a**, **1b**, and **2b** (Figure 5(A), (B), and (D), respectively) showed a complete series of sequential NH($i \rightarrow i+1$) dipolar interactions from the N-terminal N(1)H to the C-terminal N(6)H, which is characteristic of a helical secondary structure, whereas the spectrum of peptide **2a** (Figure 5(C)) showed a partial series of sequential NH($i \rightarrow i+1$) dipolar interactions except for an NH($3 \rightarrow 4$) dipolar interaction [N(3)H and N(4)H proton signals were overlapped].

CD Spectra

The CD spectra of peptides **1a**,**b** and **2a**,**b** were measured in TFE solution to obtain information about their helical screw senses. The spectra of **1a**,**b** and **2b** did not show maxima characteristic of a helical structure (approximately 208 and 222 nm; Figure 6) [40]. These results suggest that equivalent amounts of both right-handed (*P*) and left-handed (*M*) helices would be roughly existed in TFE solution. On the other hand, the CD spectrum of peptide **2a** having two internal L-Leu residues showed negative maxima at 203 and 222 nm, indicating that its helical screw sense is right handed (*P*) (Figure 6). This right-handed screw sense would be induced by two consecutive L-Leu residues. Furthermore, the ratio of *R* ($\theta_{222}/\theta_{203}$) suggests that the secondary structure of **2a** ($R = 0.2$) is a 3_{10}-helix [40].

X-ray Diffraction

Boc-L-Leu-Aib-Aib-Aib-Aib-L-Leu-OMe (**1a**) is crystallized in space group $P2_1$ to form a right-handed (*P*) 3_{10}-helix (Figure 7). The mean values of the ϕ and ψ torsion angles of the amino acid residues (1–6) were $-60.1°$ and $-27.9°$, respectively, which are close to those for an ideal right-handed (*P*) 3_{10}-helical structure ($-60°$ and $-30°$) [41–43]. Four intramolecular hydrogen bonds, which each

Table 3. Intramolecular and intermolecular H-bond parameters for **1a**, **1b**, and **2b**

Peptide[a]	Donor D-H	Acceptor A	Distance [Å] D···A	Angle [°] D-H···A	Symmetry operations
Boc-L-Leu-Aib-Aib-Aib-Aib-L-Leu-OMe (**1a**)					
	N_3–H	O_0	3.17[b]	167.4	*x*, *y*, *z*
	N_4–H	O_1	3.07	155.5	*x*, *y*, *z*
	N_5–H	O_2	2.94	153.8	*x*, *y*, *z*
	N_6–H	O_3	3.07	157.5	*x*, *y*, *z*
	N_1–H	$O_{5'}$	3.18[b]	152.7	$1-x, -1/2+y, 1-z$
	N_2–H	$O_{6'}$	3.33[b]	118.5	$1-x, -1/2+y, 1-z$
Boc-D-Leu-Aib-Aib-Aib-Aib-L-Leu-OMe (**1b**)					
	N_3–H	O_0	3.01	161.5	*x*, *y*, *z*
	N_4–H	O_1	3.06	151.5	*x*, *y*, *z*
	N_5–H	O_2	2.94	150.2	*x*, *y*, *z*
	N_6–H	O_3	3.04	161.9	*x*, *y*, *z*
	N_1–H	$O_{4'}$	2.87	141.5	$2-x, -1/2+y, -2+z$
	N_2–H	$O_{5'}$	3.15[b]	118.0	$2-x, -1/2+y, -2+z$
Boc-Aib-Aib-D-Leu-L-Leu-Aib-Aib-OMe (**2b**)					
Molecule **A**					
	N_{3a}–H	O_{0a}	3.12	142.0	*x*, *y*, *z*
	N_{4a}–H	O_{1a}	2.88	148.1	*x*, *y*, *z*
	N_{5a}–H	O_{2a}	3.15[b]	146.6	*x*, *y*, *z*
	N_{6a}–H	O_{3a}	3.13	134.8	*x*, *y*, *z*
	N_{1a}–H	$O_{4a'}$	3.07	167.7	$x, -1+y, z$
	N_{2a}–H	$O_{5a'}$	3.08	152.0	$x, -1+y, z$
Molecule **B**					
	N_{3b}–H	O_{0b}	3.00	135.6	*x*, *y*, *z*
	N_{4b}–H	O_{1b}	3.04	152.3	*x*, *y*, *z*
	N_{5b}–H	O_{2b}	3.09	141.8	*x*, *y*, *z*
	N_{6b}–H	O_{3b}	3.22[b]	135.2	*x*, *y*, *z*
	N_{1b}–H	$O_{4b'}$	2.97	169.3	$x, 1+y, z$
	N_{2b}–H	$O_{5b'}$	3.18[b]	160.0	$x, 1+y, z$

[a]The number of the amino-acid residues begins at the N-terminus of the peptide chain.
[b]The D···A distance is a bit long for a hydrogen bond.

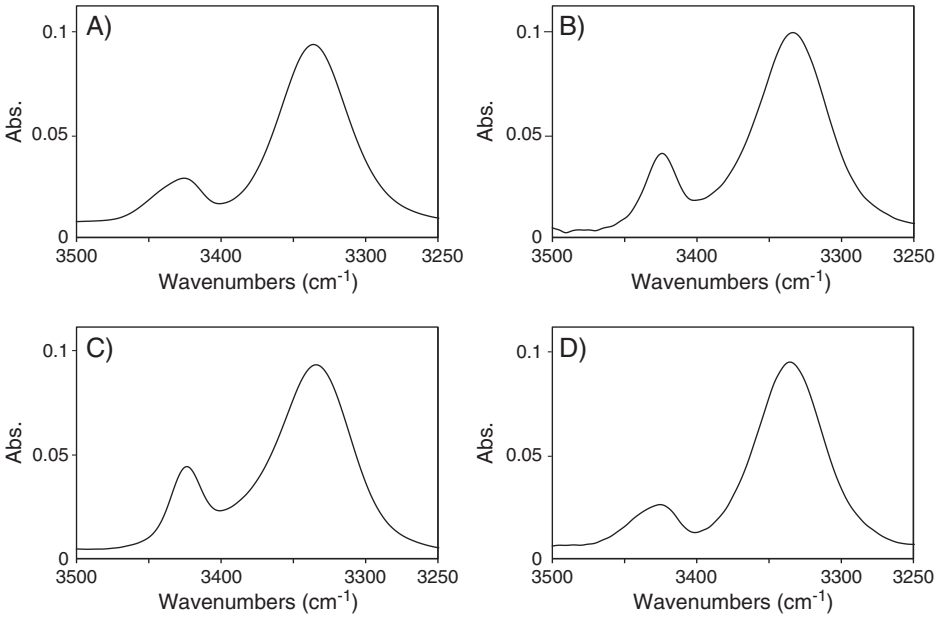

Figure 3. FT-IR spectra (3250–3500 cm^{-1} region) of peptides (A) Boc-L-Leu-Aib-Aib-Aib-Aib-L-Leu-OMe (**1a**), (B) Boc-D-Leu-Aib-Aib-Aib-Aib-L-Leu-OMe (**1b**), (C) Boc-Aib-Aib-L-Leu-L-Leu-Aib-Aib-OMe (**2a**), and (D) Boc-Aib-Aib-D-Leu-L-Leu-Aib-Aib-OMe (**2b**) at 24 °C in $CDCl_3$ solution. Peptide concentration: 1.0 mM.

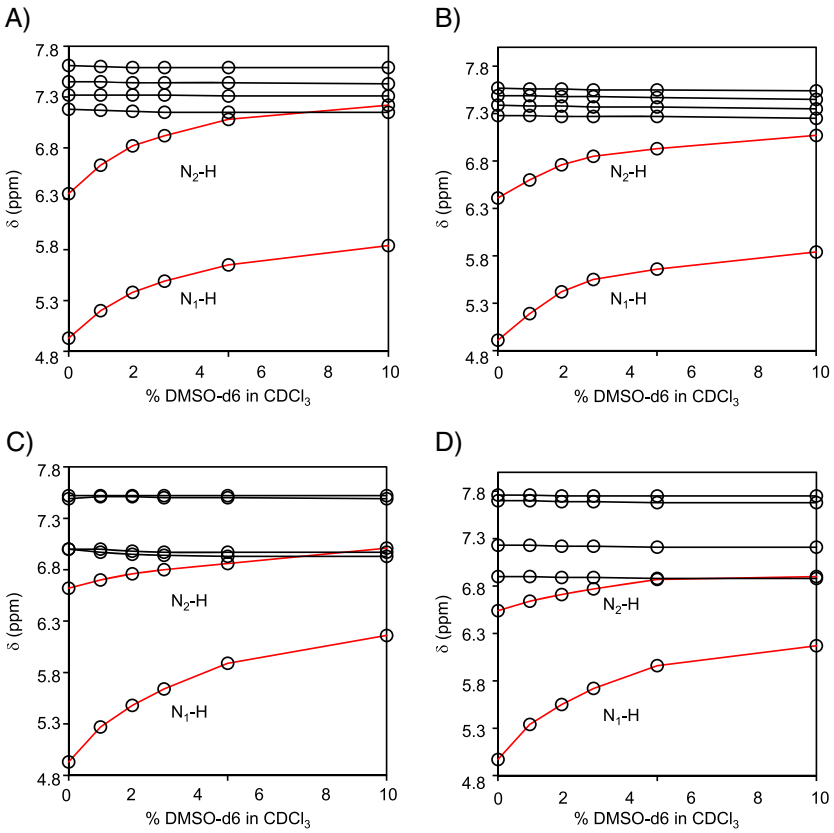

Figure 4. Plots of chemical shift values of the N–H protons of peptides (A) Boc-L-Leu-Aib-Aib-Aib-Aib-L-Leu-OMe (**1a**), (B) Boc-D-Leu-Aib-Aib-Aib-Aib-L-Leu-OMe (**1b**), (C) Boc-Aib-Aib-L-Leu-L-Leu-Aib-Aib-OMe (**2a**), and (D) Boc-Aib-Aib-D-Leu-L-Leu-Aib-Aib-OMe (**2b**) as a function of increasing percentage of DMSO-d_6 (v/v) added to the $CDCl_3$ solution at 24 °C. Peptide concentration: 1.0 mM.

form a 10-membered (atoms) pseudo ring of the $i \leftarrow i+3$ type, exist in the 3_{10}-helical molecule of **1a** [44]. They are present between the H–N(3) and C(0) = O(0) O atom of the Boc group with an N(3)···O(0) distance of 3.17 Å (which is a bit long for a hydrogen bond), between the H–N(4) and C(1) = O(1) [N(4)···O(1) = 3.07 Å], and between the H–N(5) and C(2) = O(2) [N(5)···O(2) = 2.94 Å]. The

Journal of PeptideScience

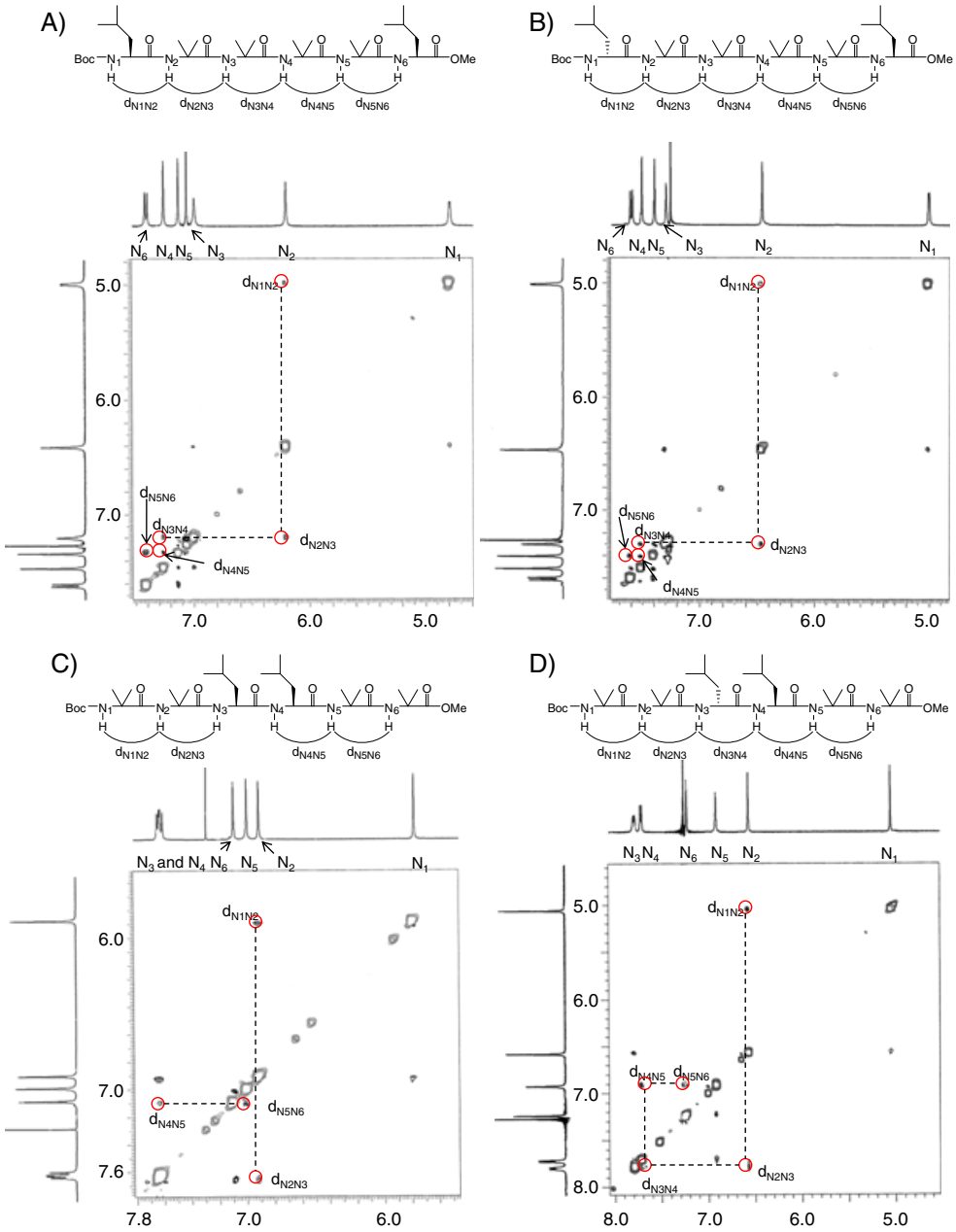

Figure 5. The nuclear Overhauser effect spectroscopy ^{1}H NMR spectra of (A) Boc-L-Leu-Aib-Aib-Aib-Aib-L-Leu-OMe (**1a**), (B) Boc-D-Leu-Aib-Aib-Aib-Aib-L-Leu-OMe (**1b**), (C) Boc-Aib-Aib-L-Leu-L-Leu-Aib-Aib-OMe (**2a**), and (D) Boc-Aib-Aib-D-Leu-L-Leu-Aib-Aib-OMe (**2b**) at 24 °C in $CDCl_3$ solution (τ_m = 200 ms). Peptide concentration: 5.0 mM.

helical molecules were connected by intermolecular hydrogen bonds, forming head-to-tail aligned chains (Figure 8).

A right-handed (*P*) 3_{10}-helix was detected in the asymmetric unit of Boc-D-Leu-Aib-Aib-Aib-Aib-L-Leu-OMe (**1b**) (Figure 9). The mean ϕ and ψ torsion angles of the amino acid residues (1–6) were −59.3° and −31.1°, respectively. Four intramolecular hydrogen bonds of the $i \leftarrow i+3$ type were present in the 3_{10}-helical molecule of **1b**. They were located between the H–N(3) and C(0) = O(0) [N(3)···O(0) = 3.01 Å], between the H–N(4) and C(1) = O(1) [N(4)···O(1) = 3.06 Å], between the H–N(5) and C(2) = O(2) [N(5)···O(2) = 2.94 Å], and between the H–N(6) and C(3) = O(3) [N(6)···O(3) = 3.04 Å]. In packing mode, the helical molecules were connected by intermolecular hydrogen bonds, forming head-to-tail aligned chains (Figure 10).

The structure of Boc-(Aib)$_2$-D-Leu-L-Leu-(Aib)$_2$-OMe (**2b**) was solved using the *P*1 space group. Two crystallographically independent molecules **A** [right-handed (*P*) 3_{10}-helix] and **B** [left-handed (*M*) 3_{10}-helix] were found to be present in the asymmetric unit (Figure 11). The mean ϕ and ψ torsion angles of the amino acid residues (1–5) were −59.9° and −36.4° for molecule **A** and +61.8° and +34.6° for molecule **B**, respectively. Reversal of the torsion angle signs of the C-terminal Aib (6) residues of molecules **A** (ϕ = +53.3°, ψ = +33.0°) and **B** (ϕ = −61.8°, ψ = −34.6°) was observed. This phenomenon is often observed in the 3_{10}-helical peptides of Aib [45]. In molecule **A**, four intramolecular hydrogen bonds of the $i \leftarrow i+3$ type were present between the H–N(3a) and C(0a) = O(0a) [N(3a)···O(0a) = 3.12 Å], between the H–N(4a) and C(1a) = O(1a) [N(4a)···O(1a) = 2.88 Å], between the H–N

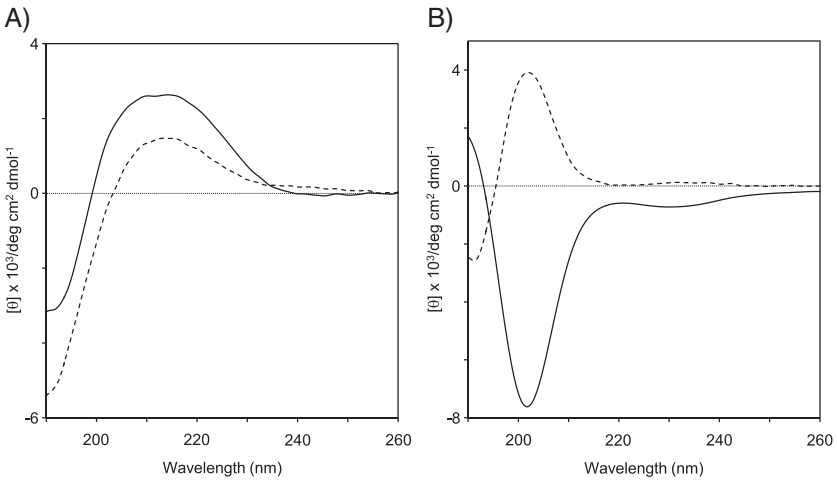

Figure 6. CD spectra in the 190–260-nm region of peptides **1a**,**b** and **2a**,**b**: (A) Boc-L-Leu-Aib-Aib-Aib-Aib-L-Leu-OMe (**1a**; solid line) and Boc-D-Leu-Aib-Aib-Aib-Aib-L-Leu-OMe (**1b**; dashed line) and (B) Boc-Aib-Aib-L-Leu-L-Leu-Aib-Aib-OMe (**2a**; solid line) and Boc-Aib-Aib-D-Leu-L-Leu-Aib-Aib-OMe (**2b**; dashed line) at 25 °C in TFE solution. Peptide concentration: 0.5 mM.

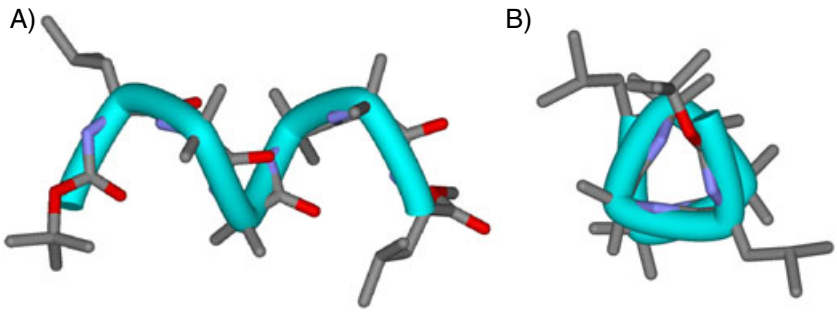

Figure 7. X-ray diffraction structures of peptide **1a** as viewed (A) perpendicular to and (B) along the helical axis.

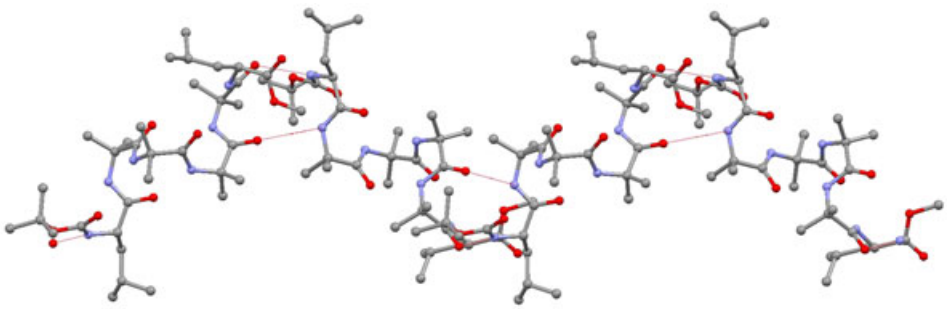

Figure 8. Packing of **1a** in the crystalline state. Intermolecular hydrogen bonds are indicated as red dashed lines.

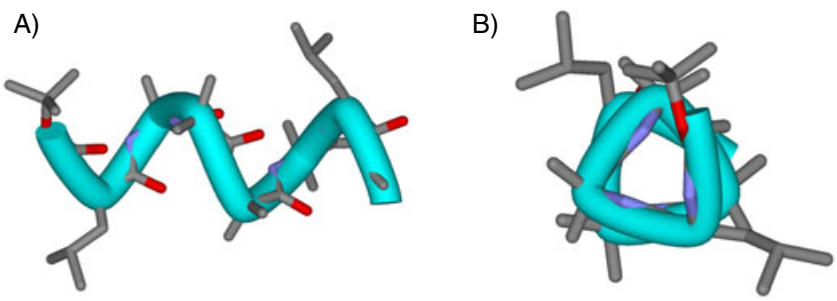

Figure 9. X-ray diffraction structures of peptide **1b** as viewed (A) perpendicular to and (B) along the helical axis.

Journal of PeptideScience

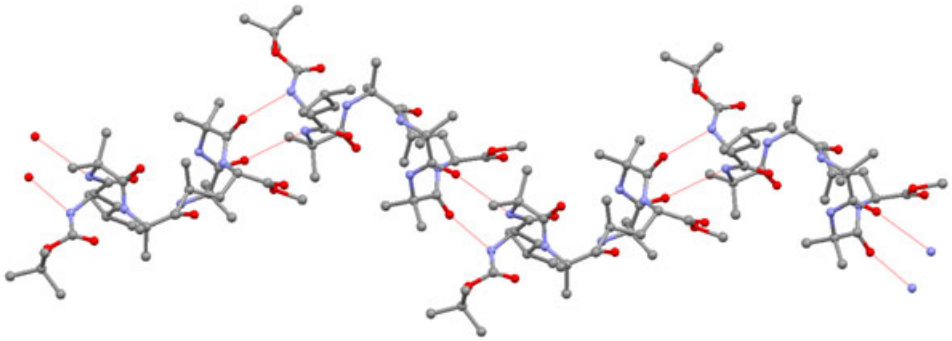

Figure 10. Packing of **1b** in the crystalline state. Intermolecular hydrogen bonds are indicated as red dashed lines.

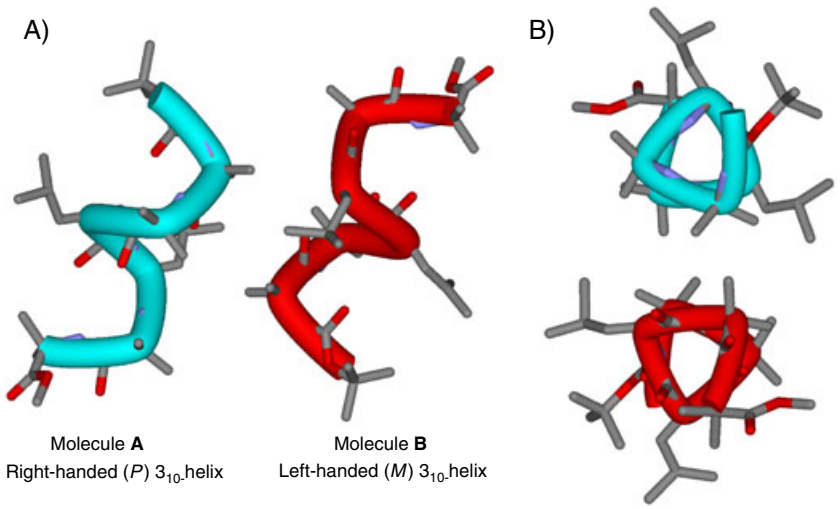

Figure 11. X-ray diffraction structures of peptide **2b** as viewed (A) perpendicular to and (B) along the helical axis.

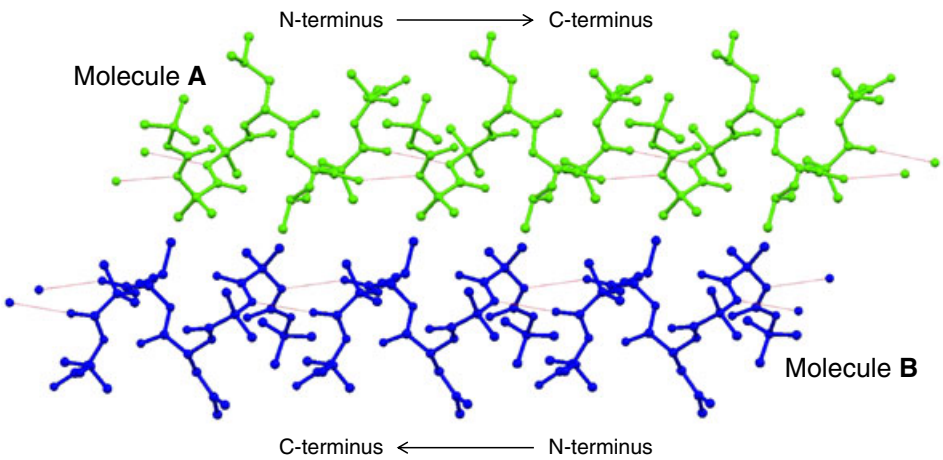

Figure 12. Packing of **2b** (green for molecule **A** and blue for molecule **B**) in the crystalline state. Intermolecular hydrogen bonds are indicated as red dashed lines.

(5a) and C(2a) = O(2a) [N(5a)···O(2a) = 3.15 Å (which is a bit long for a hydrogen bond)], and between the H–N(6a) and C(3a) O(3a) [N(6a)···O(3a) = 3.13 Å]. Molecule **B** similarly formed four intramolecular hydrogen bonds between the H–N(3b) and C(0b) = O(0b) [N(3b)···O(0b) = 3.00 Å], between the H–N(4b) and C(1b) = O(1b) [N(4b)···O(1b) = 3.04 Å], between the H–N(5b) and C(2b) = O(2b) [N(5b)···O(2b) = 3.09 Å], and between the H–N(6b) and C(3b) = O(3b) [N(6b)···O(3b) = 3.22 Å (which is a bit long for a hydrogen bond)]. The two helical molecules **A** and **B** formed chains that displayed head-to-tail alignments; i.e., ···**A**···**A**··· and ···**B**···**B**···, respectively (Figure 12).

These results indicate that, in the case of Aib-based short peptides, the attachment of a C-terminal L-Leu is more effective at controlling the helical screw sense than that of an N-terminal

L-Leu in the crystalline state; although it cannot be denied that the different conformations of peptide may occur from different crystallizing solvents. Furthermore, the ability of a central D-Leu-L-Leu segment to bestow a particular helical handedness on an achiral peptide is lower than that of an N-terminal D-Leu, C-terminal L-Leu pair. Recently, Clayden *et al.* reported that an N-terminal L-phenylalanine (L-Phe) would have a greater ability to control the helical screw sense of an achiral peptide in solution than a C-terminal L-Phe [27]. The differences between Clayden's peptides and our peptides included the type of chiral amino acids present (L-Phe and L-Leu, respectively), the types of N-terminal protecting group present (Cbz and Boc, respectively), and the peptide chain length (19 and 6 amino acid residues, respectively); therefore, these differences could be responsible for the aforementioned discrepancy. In the crystalline state, the chirality of C-terminal L-Leu would exert more control over the torsion angles of the N-terminal direction than N-terminal D-Leu chirality. Therefore, a slightly energetically favorable conformer might be preferentially packed into the crystalline conformer.

Conclusions

Four hexapeptides, Boc-L-Leu-Aib-Aib-Aib-Aib-L-Leu-OMe (**1a**), Boc-D-Leu-Aib-Aib-Aib-Aib-L-Leu-OMe (**1b**), Boc-Aib-Aib-L-Leu-L-Leu-Aib-Aib-OMe (**2a**), and Boc-Aib-Aib-D-Leu-L-Leu-Aib-Aib-OMe (**2b**), were synthesized. All hexapeptides **1a**,**b** and **2a**,**b** formed 3_{10}-helical structures by FT-IR, ^{1}H NMR, and 2D NOESY spectra in solution. The CD spectra of **1a**,**b** and **2b** did not show characteristic of helical structures. These results suggest that both right-handed (*P*) and left-handed (*M*) helices are present in the equilibrium mixtures of **1a**,**b** and **2b** in TFE solution. On the other hand, the dominant conformation of peptide **2a** was a right-handed (*P*) 3_{10}-helix. The conformations of **1a**, **1b**, and **2b** in the crystalline state were analyzed by X-ray diffraction. Right-handed (*P*) 3_{10}-helices were present in **1a** and **1b**, whereas a mixture of right-handed (*P*) and left-handed (*M*) 3_{10}-helices was present in **2b** in their crystalline states. These results provide valuable information of design and control peptide folding for structural and peptide chemists.

Acknowledgements

This work was supported in part by a Grant-in-Aid for Young Scientists (B) from the JSPS and a Kaneka Award for Synthetic Organic Chemistry, Japan.

References

1 Branden C, Tooze T. *Introduction to Protein Structure*. Garland Publishing Inc., New York, NY, 1991; 1–31.
2 Phillips C, Roberts LR, Schade M, Bazin R, Bent A, Davies NL, Moore R, Pannifer AD, Pickford AR, Prior SH, Read CM, Scott A, Brown DG, Xu B, Irving SL. Design and structure of stapled peptides binding to estrogen receptor. *J. Am. Chem. Soc.* 2011; **133**: 9696–9699.
3 Horne WS, Gellman SH. Foldamers with heterogeneous backbones. *Acc. Chem. Res.* 2008; **41**: 1399–1408.
4 Davie EAC, Mennen SM, Xu Y, Miller SJ. Asymmetric catalysis mediated by synthetic peptides. *Chem. Rev.* 2007; **107**: 5759–5812.
5 Yamagata N, Demizu Y, Sato Y, Doi M, Tanaka M, Nagasawa K, Okuda H, Kurihara M. Design of a stabilized short helical peptide and its application to catalytic enantioselective epoxidation of (*E*)-chalcone. *Tetrahedron Lett.* 2011; **52**: 798–801.
6 Demizu Y, Yamagata N, Nagoya S, Sato Y, Doi M, Tanaka M, Nagasawa K, Okuda H, Kurihara M. Enantioselective epoxidation of α,β-unsaturated ketones catalyzed by stapled helical peptides. *Tetrahedron* 2011; **67**: 6155–6165.
7 Nagano M, Doi M, Kurihara M, Suemune H, Tanaka M. Stabilized α-helix-catalyzed enantioselective epoxidation of α,β-unsaturated ketones. *Org. Lett.* 2010; **12**: 3564–3566.
8 Toniolo C, Crisma M, Formaggio F, Valle G, Cavicchioni G, Précigoux G, Aubry A, Kamphuis J. Structures of peptides from α-amino acids methylated at the α-carbon. *Biopolymers* 1993; **33**: 1061–1072.
9 Yoder G, Polese A, Silva RAGD, Formaggio F, Crisma M, Broxterman QB, Kamphuis J, Toniolo C, Keiderling TA. Conformational characterization of terminally blocked L-(αMe)Val homopepitdes using vibrational and electronic circular dichroism: 3_{10}-helical stabilization by peptide-peptide interaction. *J. Am. Chem. Soc.* 1997; **119**: 10278–10285.
10 Dehner A, Planker E, Gemmecker G, Broxterman QB, Bisson W, Formaggio F, Crisma M, Toniolo C, Kessler H. Solution structure, dimerization, and dynamics of a lipophillic $\alpha/3_{10}$-helical C^{α}-methylated peptide: implication for folding of membrane proteins. *J. Am. Chem. Soc.* 2001; **123**: 6678–6686.
11 Royo S, Borggraeve WMD, Peggion C, Formaggio F, Crisma M, Jiménez AI, Cativiela C, Toniolo C. Turn and helical peptide handedness governed exclusively by side-chain chiral center. *J. Am. Chem. Soc.* 2005; **127**: 2036–2037.
12 Tanaka M, Demizu Y, Doi M, Kurihara M, Suemune H. Chiral centers in the side chains of α-amino acids control the helical screw sense of peptides. *Angew. Chem. Int. Ed.* 2004; **43**: 5360–5363.
13 Tanaka M, Anan K, Demizu Y, Kurihara M, Doi M, Suemune H. Side-chain chiral centers of amino acid and helical-screw handedness of its peptides. *J. Am. Chem. Soc.* 2005; **127**: 11570–11571.
14 Tanaka M. Design and synthesis of chiral α,α-disubstituted α-amino acids and conformational study of their oligopeptides. *Chem. Pharm. Bull.* 2007; **55**: 349–358.
15 Demizu Y, Tanaka M, Nagano M, Kurihara M, Doi M, Maruyama T, Suemune H. Controlling 3_{10}-helix and α-helix of short peptides in the solid state. *Chem. Pharm. Bull.* 2007; **55**: 840–842.
16 Nagano M, Tanaka M, Doi M, Demizu Y, Kurihara M, Suemune H. Helical-screw directions of diastereoisomeric cyclic α-amino acid oligomers. *Org. Lett.* 2009; **11**: 1135–1137.
17 Demizu Y, Doi M, Kurihara M, Okuda H, Nagano M, Suemune H, Tanaka M. Conformational studies on peptides containing α,α-disubstituted α-amino acids: chiral cyclic α,α-disubstituted α-amino acid as an α-helical inducer. *Org. Biomol. Chem.* 2011; **9**: 3303–3312.
18 Demizu Y, Doi M, Kurihara M, Maruyama T, Suemune H, Tanaka M. One-handed helical-screw direction of homopeptide-foldamer exclusively induced by cyclic α-amino acid side-chain chiral centers. *Chem. Eur. J.* 2012; **18**: 2430–2439.
19 Benedetti E, Saviano M, Iacovino R, Pedone C, Santini A, Crisma M, Formaggio F, Toniolo C, Broxterman QB, Kamphuis J. Helical screw sense of peptide molecules: the pentapeptide system $(Aib)_4$/L-Val [L-(αMe)Val] in the crystal state. *Biopolymers* 1998; **46**: 433–443.
20 Pengo B, Formaggio F, Crisma M, Toniolo C, Bonora GM, Broxterman QB, Kamphuis J, Saviano M, Iacovino R, Rossi F, Benedetti E. Helical screw sense of peptide molecules: the pentapeptide system $(Aib)_4$/L-Val[L-(αMe)Val] in solution. *J. Chem. Soc., Perkin Trans.* 1998; **2**: 1651–1658.
21 Inai Y, Tagawa K, Takasu A, Hirabayashi T, Oshikawa T, Yamashita M. Induction of one-handed helical screw sense in achiral peptide through the domino effect based on interacting its N-terminal amino group with chiral carboxylic acid. *J. Am. Chem. Soc.* 2000; **122**: 11731–11732.
22 Inai Y, Ishida Y, Tagawa K, Takasu A, Hirabayashi T. Noncovalent domino effect on helical screw sense of chiral peptides possessing C-terminal chiral residue. *J. Am. Chem. Soc.* 2002; **124**: 2466–2473.
23 Komori H, Inai Y. Control of peptide helix sense by temperature tuning of noncovalent chiral domino effect. *J. Org. Chem.* 2007; **72**: 4012–4022.
24 Ousaka N, Inai Y, Kuroda R. Chain-terminus triggered chiral memory in an optically inactive 3_{10}-helical peptide. *J. Am. Chem. Soc.* 2008; **130**: 12266–12267.
25 Ousaka N, Inai Y. Transfer of noncovalent chiral information along an optically inactive helical peptide chain: allosteric control of asymmetry of the C-terminal site by external molecule that binds to the N-terminal site. *J. Org. Chem.* 2009; **74**: 1429–1439.
26 Clayden J, Castellanos A, Solá J, Morris GA. Quantifying end-to-end conformational communication of chirality through an achiral peptide chain. *Angew. Chem. Int. Ed.* 2009; **48**: 5962–5965.

27 Solá J, Helliwell M, Clayden J. N- versus C-terminal control over the screw-sense preference of the configurationally achiral, conformationally helical peptide motif $Aib_8GlyAib_8$. *J. Am. Chem. Soc.* 2010; **132**: 4548–4549.
28 Solá J, Fletcher SP, Castellanos A, Clayden J. Nanometer-range communication of stereochemical information by reversible switching of molecular helicity. *Angew. Chem. Int. Ed.* 2010; **49**: 6836–6839.
29 Brown RA, Marcelli T, Poli MD, Solá J, Clayden J. Induction of unexpected left-handed helicity by an N-terminal L-amino acid in an otherwise achiral peptide chain. *Angew. Chem. Int. Ed.* 2012; **51**: 1395–1399.
30 Boddaert T, Solá J, Helliwell M, Clayden J. Chemical communication: conductors and insulators of screw-sense preference between helical oligo(aminoisobutyric acid) domains. *Chem. Commun.* 2012; **48**: 3397–3399.
31 Solá J, Morris GA, Clayden J. Measuring screw-sense preference in a helical oligomer by comparison of ^{13}C NMR signal separation at slow and fast exchange. *J. Am. Chem. Soc.* 2011; **133**: 3712–3715.
32 Demizu Y, Yamagata N, Sato Y, Doi M, Tanaka M, Okuda H, Kurihara M. Controlling the helical screw sense of peptides with C-terminal L-valine. *J. Pept. Sci.* 2010; **16**: 153–158.
33 Demizu Y, Tanaka M, Doi M, Kurihara M, Okuda H, Suemune H. Conformations of peptides containing a chiral cyclic α,α-disubstituted α-amino acid within the sequence of Aib residues. *J. Pept. Sci.* 2010; **16**: 621–626.
34 Demizu Y, Doi M, Sato Y, Tanaka M, Okuda H, Kurihara M. Three-dimensional control of diastereomeric Leu-Leu-Aib-Leu-Leu-Aib sequences in the solid state. *J. Org. Chem.* 2010; **75**: 5234–5239.
35 Demizu Y, Doi M, Sato Y, Tanaka M, Okuda H, Kurihara M. Screw-sense control of helical oligopeptides containing equal amounts of L- and D-amino acids. *Chem. Eur. J.* 2011; **17**: 11107–11109.
36 Demizu Y, Doi M, Sato Y, Tanaka M, Okuda H, Kurihara M. Effect of one D-Leu residue on right-handed helical -L-Leu-Aib- peptides in the crystal state. *J. Pept. Sci.* 2011; **17**: 420–426.
37 Sheldrick GM. A short history of SHELX. *Acta Cryst.* 2008; **A64**: 112–122.
38 Sheldrick GM. *Program for Crystal Structure Refinement (SHELXL 97)*. University of Göttingen: Göttingen, 1997.
39 Kennedy DF, Crisma M, Toniolo C, Chapman D. Studies of peptides forming 3_{10}- and α-helices and β-bend ribbon structures in organic solution and in model biomembranes by Fourier transform infrared spectroscopy. *Biochemistry* 1991; **30**: 6541–6548.
40 Toniolo C, Polese A, Formaggio F, Crisma M, Kamphuis J. CD spectrum of a peptide 3_{10}-helix. *J. Am. Chem. Soc.* 1996; **118**: 2744–2745.
41 Liskamp RMJ. Conformationally restricted amino acids and dipeptides, (non)peptidomimetics and secondary structure mimetics. *Recl. Trav. Chim. Pays-Bas.* 1994; **113**: 1–19.
42 Pal L, Basu G, Chakrabarti P. Variants of 3_{10}-helices in proteins. *Proteins: Struct. Funct. Genet.* 2002; **48**: 571–579.
43 Toniolo C, Benedetti E. The polypeptide 3_{10}-helix. *Trends Biochem. Sci.* 1991; **16**: 350–353.
44 Görbitz CH. Hydrogen-bond distances and angles in the structures of amino acids and peptides. *Acta Crystallogr.* 1989; **B45**: 390–395.
45 Benedetti E, Bavoso A, Di Blasio B, Pavone V, Pedone C, Crisma M, Bonora GM, Toniolo C. Solid-state and solution conformation of homooligo(α-aminoisobutyric acids) from tripeptide to pentapeptide: evidence for a 3_{10}-helix. *J. Am. Chem. Soc.* 1982; **104**: 2437–2444.

